IEICE The Institute of Electronics, Information and Communication Engineers

IEICE Proceeding Series

Range Finding and Fault Locating with Chaotic Signal

An-Bang Wang, Tong Zhao, Hang Xu, Na Wang, Yun-Cai Wang

Vol. 1 pp. 458-461
Publication Date: 2014/03/17
Online ISSN: 2188-5079

2012 International Symposium on Nonlinear Theory and its Applications
NOLTA2012, Palma, Majorca, Spain, October 22-26, 2012

Range Finding and Fault Locating with Chaotic Signal

An-Bang Wang, Tong Zhao, Hang Xu, Na Wang and Yun-Cai Wang

The Key Laboratory of Advanced Transducers and Intelligent Control System, Ministry of Education of China
College of Physics and Optoelectronics, Taiyuan University of Technology, Taiyuan 030024, China
Email: wanganbang@tyut.edu.cn, zhaot321@yahoo.com.cn, wangyc@tyut.edu.cn

Abstract– In this paper, we review our recent works on range finding and fault locating in optical network and wire with chaotic signal. Using a distributed-feedback semiconductor laser with optical feedback as chaotic source, we developed a prototype chaotic optical time domain reflectometer which can achieve a range-independent resolution of 4cm and measurable distance of about 70km. We further present the measurement of faults in the wavelength-division-multiplexing passive optical network (WDM-PON) by using a wavelength-tunable chaotic laser. Moreover, we also demonstrate the location of wire faults or impedance discontinuities with chaotic signal. Our results show that the fault location using wideband chaotic signal is a promising method of precise diagnoses for WDM-PON and electric cables.

1. Introduction

Optical time domain reflectometer (OTDR) [1] and time domain reflectometer (TDR) [2] have been important diagnostic tools for fault detection on single fiber link and wire, respectively. Further, wavelength-tunable OTDR [3] has been used to diagnostic the wavelength-division-multiplexing passive optical network (WDM-PON). They all utilize a single optical or electric pulse as probe signal, and achieve measurement by detecting the power and arriving time of the echo pulse. However, there is a tradeoff between spatial resolution and measurable range. Generally, their spatial resolutions which are determined by the pulse duration are about tens of meters. Ultra-short optical or electric pulse technique can improve spatial resolution, but it needs assistance from other expensive and complicated techniques to enlarge signal-to-noise ratio [4]. To solve this problem, the correlation OTDR [5], wavelength-tunable correlation OTDR [6], and sequence time domain reflectometer (STDR) [7] have been presented. They employ a pseudo-random sequence and pseudo-random optical pulse sequence instead of single pulse as probe signal. It overcomes the tradeoff by increasing sequence length to improve the energy of probe signal rather than by widening pulse. However, without expensive high-speed pseudo-random sequence generator and wideband modulator, the resolution is also limited to tens of meters [8] by the code width of the sequence.

Remarkably, wideband chaotic signal spreading over several gigahertz can be readily obtained from a laser diode [9]. In particular, its waveform has an ideal thumbtack ambiguity function, and thus has been proposed for lidar applications [10]. Hence, our group has proposed chaotic optical time domain reflectometry (COTDR) [11], wavelength-tunable COTDR [12] and subsequently developed it to detect wiring faults [13]. In this paper, we review our recent works on range finding and fault locating in optical network and wire with chaotic signal. Our works mainly consists of three aspects involving COTDR, wavelength-tunable COTDR, and location of wire faults using chaotic signal. In the following sections, they will be demonstrated respectively.

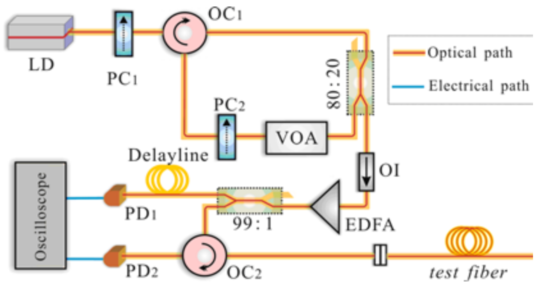

Fig. 1. Experimental setup of the proposed COTDR. PC: polarization controller; OC: optical circulator; EDFA: erbium-doped fiber amplifier; VOA: variable optical attenuator; PD: photodetector.

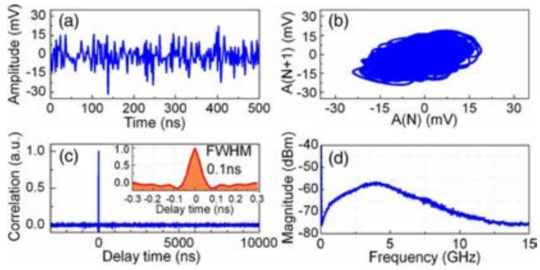

Fig.2. Properties of the chaotic signal. (a) Temporal waveform. (b) Attractor. (c) Autocorrelation trace. (d) Power spectrum.

2. Range Finding and Fault locating

2.1. Chaotic Optical Time Domain Reflectometer (COTDR)

The experimental setup of the proposed COTDR is shown in Fig. 1. The chaotic source is a laser diode with optical feedback from an external fiber ring cavity consisting of an optical circulator OC1, a variable optical attenuator (VOA) and polarization controllers (PC1, PC2). The feedback strength and polarization are adjusted and controlled by VOA and polarization controllers,

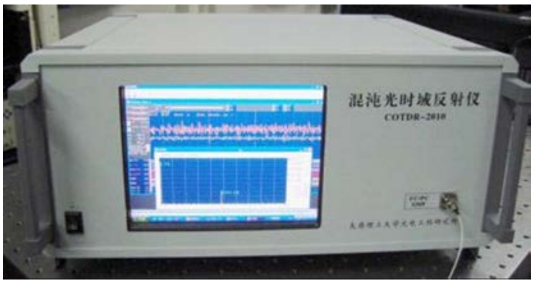

Fig.3. Photo of COTDR prototype.

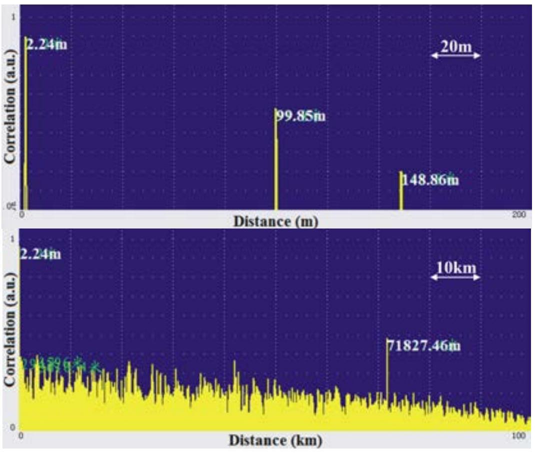

Fig.4. The experimental results of (a) the fiber connector and breakpoint, and (b) the breakpoint at 72km measured by the COTDR.

respectively. After an optical isolator, the chaotic laser output is amplified by an erbium-doped fiber amplifier (EDFA), and then is split by a 99:1 fiber coupler, which provides 1% of the laser output for the reference light and 99% for the probe light. The probe light is launched into the tested fiber and its reflected light is received through optical circulator OC2. To minimize the difference, both the echo probe light and reference light are converted into electrical signals by two identical photodetectors and recorded by a real-time oscilloscope. The correlation between the reference and the echo light can be calculated by using a computer, thus we can locate the fault events in fibers by the correlation peak.

Figure 2 shows the properties of the chaotic signal from laser diode, which was generated with −20dB and 30ns of feedback. Fig. 2(a)-(c) respectively show the waveform, attractor, and autocorrelation curve. Obviously, the chaotic waveform varies rapidly and irregularly, and its ergodic attractor further indicates its randomness. Furthermore, the delta-profile curve in Fig. 2(c) shows that the chaotic signal is non-periodic and has only a correlation with itself. The inset shows the full width at half maximum (FWHM) of the correlation peak which is 0.1 ns. In addition, the chaotic signal spreads over 10 GHz in frequency domain, as shown with power spectrum in Fig.2 (d), which is measured with a 47-GHz detector and a spectrum analyzer.

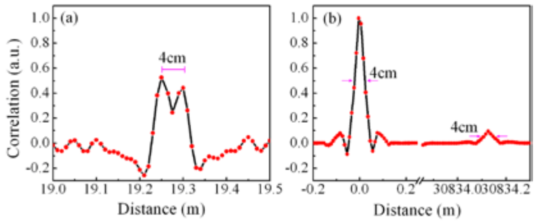

Fig.5. Spatial resolution of 4cm. (a) Identification of two reflection events with 4-cm spacing, and (b) a measurement of a long fiber with open end to show the resolution is independent of distance.

According to this experiment setup, we have developed a prototype COTDR, as shown in Fig. 3. Fig. 4 (a) displays the experimental results of the fiber connector and breakpoint measured by the COTDR. We constructed a link using two fibers with length of about 100m and 50m connected by a mated FC/PC connector, and broke the fiber link at the end. In Fig. 4 (a), the first correlation peak at 2.24m is induced by the reflection of the connected launch port. The test of correlation peaks shows the connector and breakpoint, which are located at 99.85m and 148.86m. Figure 4(b) shows the detection result of a long fiber with length of more than 70km was installed with open end. The correlation peak reads the distance as 71 827.46m.

The spatial resolution is determined by the width of correlation peak and, if according to –3-dB criterion, equals $v \cdot \text{FWHM}/2$, where v is the propagation velocity of the chaotic signal. The FWHM is determined by the bandwidth of the recorded chaotic signal in principle, and the higher the bandwidth, the narrower the correlation peak is. As shown in Fig. 5(a), two peaks with 4-cm spacing can be clearly identified. Furthermore, we use a measurement result of a fiber endpoint with distance of more than 30km plotted in Fig. 5(b) to show that the resolution is independent of distance. The first peak at reference zero point has a FWHM of 4cm, and the correlation peak at 30 834.13m has the same FWHM although the round-trip propagation of the probe light is over 60km. This means the spatial resolution of 4cm does not vary with the position of fault.

2.2. Wavelength-tunable COTDR

In Fig. 6, we show the experimental setup of the proposed wavelength-tunable COTDR, including two units of light source and detection. In the light source unit, the wavelength-tunable chaotic light source is a multiple-longitudinal-modes FP laser subject to filtered optical feedback, plotted in the top dashed box. The FP laser operates in the 1.55um band and has about 30 longitudinal modes with spacing of 1.2nm. Its modes can be tuned by a temperature controller to be compatible with the WDM channels with 50GHz spacing recommended by International Telecommunication Union (ITU) with

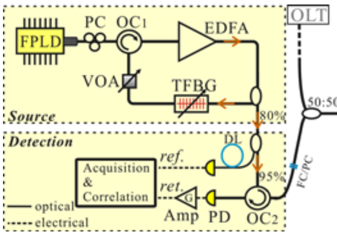

Fig.6. Experimental setup of the proposed wavelength-tunable COTDR. PC: polarization controller; OC: optical circulator; EDFA: erbium-doped fiber amplifier; TFBG: tunable fiber Bragg grating; VOA: variable optical attenuator; PD: photodetectors; Amp: electrical amplifier; AWG: arrayed waveguide grating; DL: delay line.

G.694.1 standard. After going through an erbium-doped fiber amplifier (EDFA), the laser emission is divided by a fiber coupler into two paths: one (80%) is used as output and the other as feedback light. In the feedback path, a tunable fiber Bragg grating (TFBG) with –3-dB linewidth of about 0.2nm is employed to select one mode of the laser which will partly return into laser cavity. The feedback strength is controlled by the following variable optical attenuator (VOA). In addition, the polarization of feedback light is adjusted to match that of the laser by a polarization controller. By tuning the grating wavelength and the feedback strength, one can obtain a wavelength-tunable single-mode output with chaotic intensity fluctuation. In the detection unit, the chaotic light from the source is split into two beams by a 5:95 fiber coupler, the beam from 95% port serving as probe light and the other as reference. The probe light is launched and received by an optical circulator OC2, which is connected with a 3-dBcoupler on the feeder line in the WDM-PON under test. By sweeping the wavelength of chaotic probe light, each branch link can be diagnosed by turns. The acquisition and calculation of the return light induced by faults and the reference light are similar to the COTDR.

Fig. 7 (a)-(d) shows the measured curves for channels at 1546.92, 1548.11, 1549.32, and 1550.52nm, respectively. In Fig. 7(a), the first correlation peak at zero point is induced by the reflection of the connected launch port. The following part of the correlation curve included in the dashed box is magnified in the inset. The peak at 10.35m is caused by the reflection of the AWG. The second peak at 11.49m in the inset is due to the connector following the AWG. Fig. 7(a) also displays a measure result of an opened FC/PC connector which is located at distance of 107.59m with reflection strength of −14.6dB. In the channel of 1548.11nm, a long fiber with length of more than 10km was installed with open end. Fig. 7(b) shows the detection result of this fiber endpoint which is located at 10 380.96m with reflection strength of −15.6dB. In channel of 1549.32nm, two fibers with length of about 6 and 20km, respectively, were jointed by a loose FC/PC connector, and the fiber end was open. In channel of 1550.52nm, we constructed a link using two fibers with length of about 5 and 10km connected by a mated FC/PC connector, and broke the fiber link at about 200m before its end. As shown in Fig. 7(c), one can find two reflection events in channel of 1549.32nm, which are located at 6 166.95 and 25 762.18m with reflection strengths of −24.6 and −16.8dB. As depicted in Fig. 7(d), there are also two events in the channel of 1550.52nm occurring at 5 133.09 and 15 399.33m, with reflection strengths of −32.1 and −30dB.

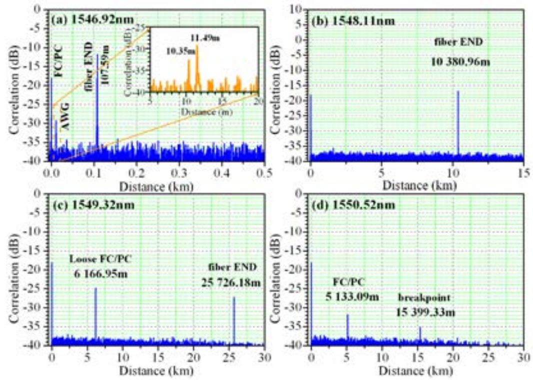

Fig.7. Experimental measure results for channels at wavelength of (a) 1546.92nm, (b) 1548.11nm, (c) 1549.32nm, and (d) 1550.52nm.

2.3. Location of Wire Faults Using Chaotic Signal

The principle of detecting faults in wires is similar to COTDR. The difference is that the launched signal is an electrical signal. In our experiments, it is obtained from chaotic laser by optoelectronic conversion. The simpler method is the use of a chaotic circuit.

Fig. 8(a) shows the detection of an open circuit for 50Ω coax with a length of 11.1m, and the inset lists the characteristics of the tested cable (Belden URM43). The base peak is the scaling zero of measurements in Fig. 8(a). Then, the first correlation peak on the right of the base peak reads the location of this breakpoint. In addition, the two shorter peaks standing at 22.2 and 33.3m are harmonic response to the second and third reflections of breakpoint, respectively. Fig. 8(b) shows the diagnosis of impedance mismatch and type. The inset shows the wiring topology which includes the three connection points, namely, A, B, C, and a 50Ω load at the terminal. The cables except in the segment of BC were still the 50Ω URM43 coax. We separately inserted a (75±5)Ω coax of 10.6m, a (100±15)Ω UTP Ethernet cable of 10.1m, and a (140±20)Ω telephone wire of 10.4m in BC. Three peaks appearing in each trace read the location of three points are shown as traces (a)–(c). In particular, the peaks at B and C are in opposite directions and, thus, indicate reflections with opposite polarity. Such results accord with the prediction of reflection coefficient $\Gamma = (Z_L - Z_0)/(Z_L + Z_0)$, where Z_0 and Z_L are the impedances of the cable and discontinuity, respectively. By calculating the reflection coefficient, we can obtain the impedances of discontinuity *B* of 78, 112, and 149Ω, within the nominal values. Similarly, we also detected the impedance at connector *A* of 56.8Ω.

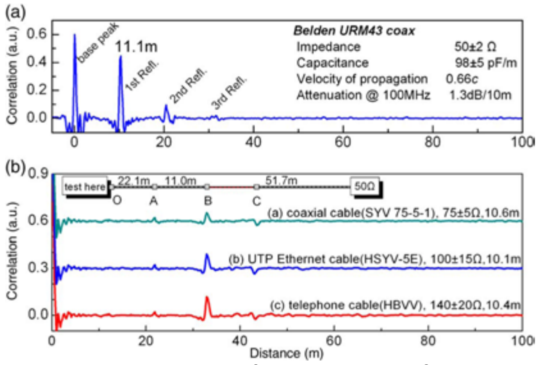

Fig.8. Experimental results of locating wiring faults. (a) Open circuit at 11.1 m. (b) Impedance mismatch.

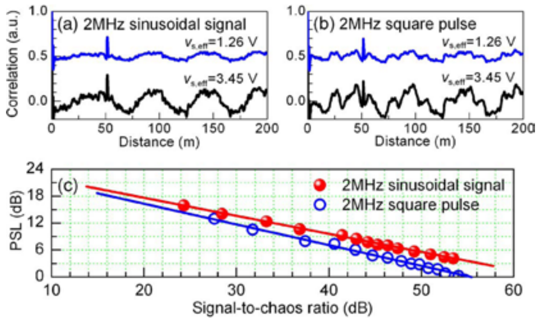

Fig. 9. (a) Experimental live test for a 2-MHz sinusoidal signal on cable: The upper and lower traces were obtained with the signal's effective voltages of 1.26 and 3.45V, respectively. (b) Results for 2-MHz square pulse. (c) PSL as a function of SCR.

Figure 9(a) show the detection results of an open-circuit point at a distance of 50m on a live wire (BeldenURM43), which separately carried a 2-MHz sine wave and a 2-MHz square signal with a duty cycle of 50%. In Fig. 9(a)-(b), the fault was apparently located in both cases. As expected, the correlation traces were influenced by the reflected sine wave and square signal: The modulation period of about 50m just corresponds to the frequency of 2MHz, and the modulation depth increases as the signal power rises. Fig. 9(c) shows the peak sidelobe level (PSL) as a function of the signal-to-chaos (SCR) of the sinusoidal and square signal. The SCR is defined as $20\log_{10}(v_{s,eff}/v_{c,eff})$, where $v_{s,eff}$ and $v_{c,eff}$ are effective voltage of existing signal and chaotic probe signal, respectively. The PSL is defined as the ratio of the correlation peak to its maximum sidelobe. Although the PSL decreases linearly with the increment of SCR, it is beyond 3dB until the SCR increases to 50dB for the square pulse or to 56dB for the sinusoidal signal. The proposed method, therefore, can detect faults with very small chaotic signal compared with the existing signal, which is less than the general noise margin.

3. Conclusions

In summary, we have proposed a chaotic OTDR for fiber faults location, and developed a prototype. Further, a tunable COTDR for WDM-PON and chaotic TDR for wiring faults were presented and demonstrated. Our previous results show that the use of chaotic signal can realize a range-independent resolution of about 4cm. It is reasonably believed that these methods are promising candidate for diagnosing WDM-PON and electric cables.

Acknowledgments

This work was supported in part by the National Natural Science Foundation of China (Grant No. 60908014 and 60777041) and in part by the Natural Science Foundation for Young Scientists (Grant No. 2009021003) and the Key Science and Technology Program (Grant No. 20100321055-02) of Shanxi Province, China.

References

[1] P. Healey, "Instrumentation principles for optical time domain reflectometry," *J. Phys E: Sci Instrum.*, vol.19, pp.334-341, 1986.
[2] N. G. Paulter, "Long-term repeatability of a TDR-based printed wiring board dielectric constant measurement system," *IEEE Trans. Instrum. Meas.*, vol. 47, pp. 1469-1473, 1998.
[3] K. Tanaka *et al.*, "Measuring the individual attenuation distribution of passive branched optical networks," *IEEE Photon. Technol. Lett.*, vol. 8, pp. 915-917, 1996.
[4] M. Legr´e *et al.*, "High resolution optical time domain reflectometer based on 1.55 m up-conversion photon-counting module," *Opt. Exp.*, vol.15, pp. 8237-8242, 2007.
[5] M. Nazarathy *et al.*, "Real-time long range complementary correlation optical time domain reflectometer," *J. Lightw. Technol.*, vol.7, pp. 24-38, 2004.
[6] J. Lee *et al*, "In-service monitoring of 16 port x 32 wavelength bi-directional WDM-PON systems with a tunable, coded optical time domain reflectometry," *Opt. Exp.*, vol. 15, pp. 6874-6882, 2007.
[7] C. R. Sharma *et al*, "Low-power STDR CMOS sensor for locating faults in aging aircraft wiring," *IEEE J. Sens.*, vol. 7, pp. 43-50, 2007.
[8] J. Lee *et al.*, "In-service monitoring of 16 port x 32 wavelength bi-directional WDM-PON systems with a tunable, coded optical time domain reflectometry," *Opt. Exp.*, vol. 15, pp. 6874-6882, 2007.
[9] A. Uchida *et al.*, "High-frequency broadbandsignal generation using a semiconductor laser with a chaotic optical injection," *IEEE J. Quantum Electron.*, vol. 39, pp. 1462-1467, 2003.
[10] F. Y. Lin *et al.*, "Chaotic lidar," *IEEE J. Sel. Topics Quantum Electron.*, vol. 10, pp. 991-997, 2004.
[11] Y. C. Wang *et al.*, "Chaotic correlation optical time domain reflectometer utilizing laser diode," *IEEE Photon. Technol. Lett.*, vol.20, pp.1636-1638, 2008.
[12] A. B Wang *et al.*, "Precise Fault Location in WDM-PON by Utilizing Wavelength Tunable Chaotic Laser," submitted to *J. Lightw. Technol.*, 2012.
[13] A. B Wang *et al.*, "Location of wire faults using chaotic signal," *IEEE Electron Device Lett.*, vol. 32, pp. 372-374, 2011.